Protist, Vol. 150, 149–162, August 1999 © Urban & Fischer Verlag
http://www.urbanfischer.de/journals/protist



ORIGINAL PAPER

# Ultrastructure of *Trimastix pyriformis* (Klebs) Bernard et al.: Similarities of *Trimastix* Species with Retortamonad and Jakobid Flagellates

**Charles J. O'Kelly[a,1], Mark A. Farmer[b], and Thomas A. Nerad[c]**

[a] Bigelow Laboratory for Ocean Sciences, West Boothbay Harbor, Maine 04575, USA
[b] Center for Advanced Ultrastructural Research, University of Georgia, Athens, Georgia 30602, USA
[c] Protistology Department, American Type Culture Collection, Manassas, VA 20110-2209, USA

Submitted March 10, 1999; Accepted May 31, 1999
Monitoring Editor: Michael Melkonian

***Trimastix pyriformis* (Klebs 1893) Bernard et al. 1999, is a quadriflagellate, free-living, bacterivorous heterotrophic nanoflagellate from anoxic freshwaters that lacks mitochondria. Monoprotist cultures of this species contained naked trophic cells with anterior flagellar insertion and a conspicuous ventral groove. Bacteria were ingested at the posterior end of the ventral groove, but there was no persistent cytopharyngeal complex. The posterior flagellum resided in this groove, and bore two prominent vanes. A Golgi body (dictyosome) was present adjacent to the flagellar insertion. The kinetid consisted of four basal bodies, four microtubular roots, and associated fibers and bands. Duplicated kinetids, each with four basal bodies and microtubular root templates, appeared at the poles of the open mitotic spindle. *Trimastix pyriformis* is distinguishable from other *Trimastix* species on the basis of external morphology, kinetid architecture and the distribution of endomembranes. *Trimastix* species are most similar to jakobid flagellates, especially *Malawimonas jakobiformis*, and to species of the retortamonad genus *Chilomastix*. Retortamonads may have evolved from a *Trimastix*-like ancestor through loss of "canonical" (easily seen with electron microscopy) endomembrane systems and elaboration of cytoskeletal elements associated with the cytostome/cytopharynx complex.**

## Introduction

Until recently, knowledge of *Trimastix*, a genus of quadriflagellate heterotrophic nanoflagellates from anoxic waters, was restricted to the light-microscope descriptions of Kent (*Trimastix marina*, the type species; Kent 1880) and Hollande (*T. convexa* Hollande in Grassé 1952). Brugerolle and Patterson (1997) redescribed *T. convexa* at the light and elec-

[1] Corresponding author;
fax 1-207-633-9641
e-mail cokelly@bigelow.org

**Abbreviations:** 1, posterior (presumed elder) basal body/flagellum; 2, anterior (presumed younger) basal body/flagellum; 3, (presumed) younger basal body associated with basal body 2; 4, (presumed) younger basal body associated with basal body 1; A, A fiber of kinetid; An, microtubular root associated with basal body 2; B, B fiber of kinetid; C, C fiber of kinetid; D, dorsal side of cell; FV, food vacuole; G, Golgi stack (dictyosome); I, I fiber of kinetid; L, left ventral microtubular root, also left side of cell; R, right ventral microtubular root, also left side of cell; $R_i$, inner subunit of R; $R_o$, outer subunit of R; S, singlet ventral microtubular root; scm, microtubule fan emanating from An; V, ventral side of cell.

1434-4610/99/150/02-149 $ 12.00/0

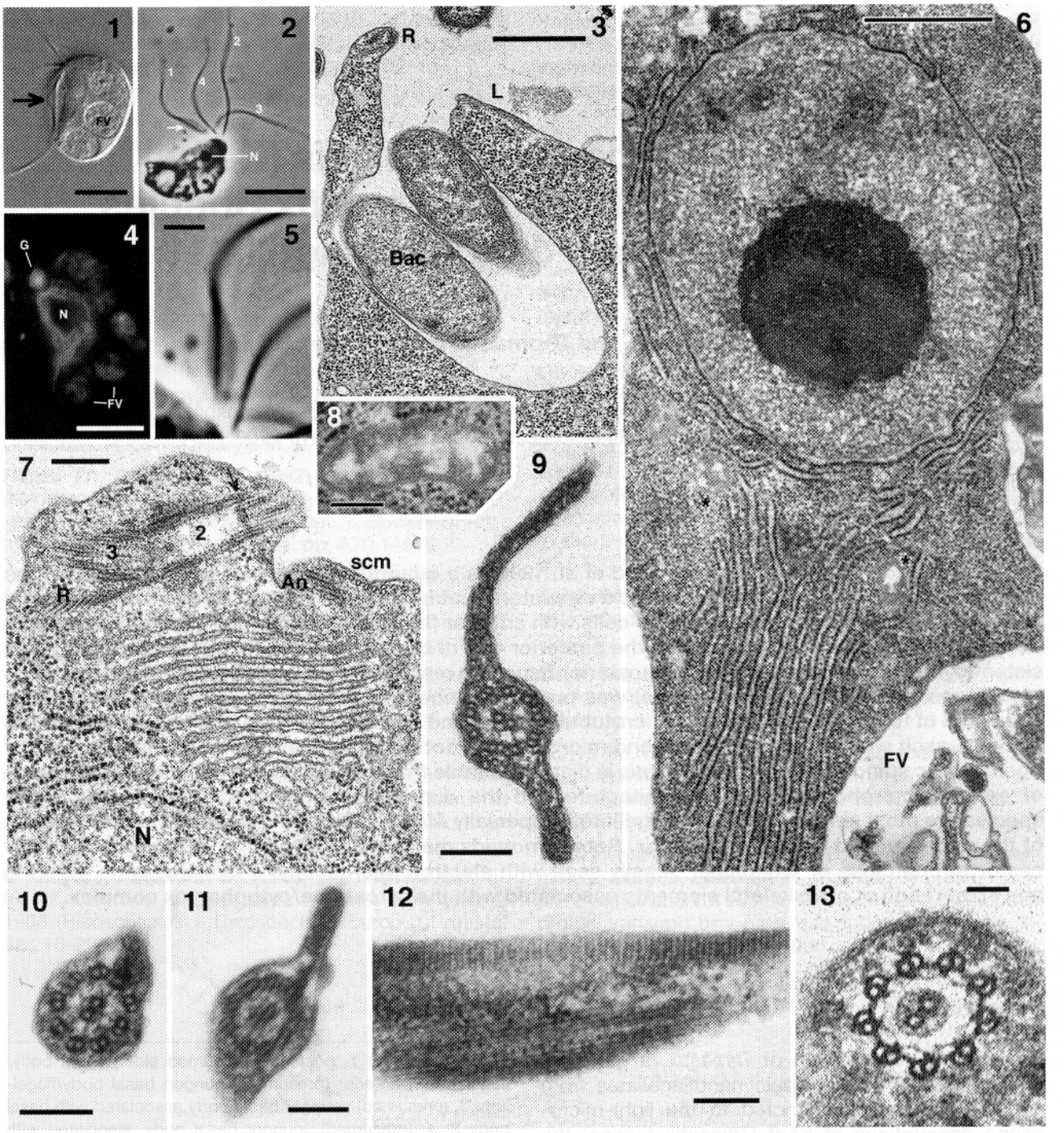


**Figures 1–13.** *Trimastix pyriformis* flagellate cells: light, fluorescence and transmission electron (TEM) micrographs. **Figure 1.** A live cell in lateral view, showing the overall shape of the cell, the posterior flagellum lying within and extending beyond the ventral groove, and food vacuoles. Vanes are visible on the posterior flagellum (arrow). Differential interference contrast. Strain 50598. Scale bar = 5 μm. **Figure 2.** A cell fixed for TEM, showing the four flagella and their relative lengths, as well as the proximal vanes on the posterior flagellum (arrow). Phase contrast. Strain 50598. Scale bar = 5 μm. **Figure 3.** TEM section near the posterior end of the ventral groove, showing partially engulfed bacteria. Microtubules from the left and right ventral roots define the margins of the groove. Strain 50562. Scale bar = 250 nm. **Figure 4.** Fluorescence micrograph of a fixed cell incubated in BODIPY ceramide, cell orientation as in Figure 1. Fluorescence signals correspond to the position of the Golgi dictyosome and the rough

tron microscope levels. They rejected the assignment of *Trimastix* to the trichomonads, as proposed by Grassé (1952; see also Cavalier-Smith 1996–97, 1998), and treated it as a unique taxon, with some resemblance to the retortamonads and the heteroloboseans. Bernard et al. (1999), in a survey of free-living flagellates from anoxic habitats, rediscovered *T. marina*, transferred *Tetramitus pyriformis* Klebs 1893 to *Trimastix*, placed *T. convexa* in synonymy with *T. pyriformis*, and described a new species, *T. inaequalis*. The ultrastructural features of *T. marina* are under investigation (AGB Simpson, personal communication).

In these recent studies, comparisons have been made between *Trimastix* and both retortamonads and heteroloboseans. None, though, have been made with the jakobid flagellates, which also have features resembling retortamonads (O'Kelly 1993, 1997; O'Kelly and Nerad 1999) and may be among the most ancient of mitochondrial eukaryotes (Gray et al. 1998, 1999; Lang et al. 1997, 1998; O'Kelly 1993).

In this paper, the ultrastructure of *Trimastix pyriformis* is described from two cultured strains. The observed features closely resemble those in *Trimastix convexa*, but sufficient differences exist to recognize two species. The features of *Trimastix* species are compared with those of other protists. Similarities between these species and those of the jakobids and retortamonads suggest a close phylogenetic relationship among these groups.

## Results

### Interphase Cell Structure

Flagellate cells were malleable in shape in response to culture conditions, availability of prey bacteria, and contact with surfaces. In general, they were rounded to elongate, with a convex dorsal surface and a planar to concave ventral surface (Figs. 1–2). Both the anterior and posterior ends of the cells were blunt-ended, without posterior spikes or other prolongations. The ventral surface of a healthy cell was dominated by a groove, which extended at least two-thirds the length of the cell (Fig. 1). The insertion of the flagella at the head of this groove, but below the cell apex, gave the cells a "hunched" appearance. Bacteria were captured at the posterior end of the groove and wound up in food vacuoles distributed in the posterior two thirds of the cell (Figs. 1, 3–4), but no permanently-differentiated cytostome or cytopharynx was observed.

The anteriormost of the four flagella (by convention, labelled "2") was slightly longer than the others, at ca. twice the length of the cell body. The other flagella were approximately equal in length, at ca. 1.5 times the cell body length (Fig. 2). The posterior flagellum (by convention, "1") resided in the ventral groove and projected from its posterior end (Fig. 1). This flagellum possessed two vanes at its proximal end, which were especially visible when the flagellum was dislodged from the groove, as sometimes

endoplasmic reticulum surrounding and posterior to the nucleus. Food vacuoles also fluoresce. Fluorescence is absent in unstained controls (not shown). Compare Figs. 6, 7. Strain 50562. Scale bar = 5 μm. **Figure 5.** Detail of Fig. 2 showing posterior flagellar vanes. Scale bar = 2 μm. **Figure 6.** TEM section through the midregion of the cell, showing the nucleus with its central nucleolus and rough endoplasmic reticulum surrounding the nucleus and extending towards the cell posterior. Presumptive hydrogenosomes are present (asterisks), as are food vacuoles. Strain 50598. Scale bar = 1.0 μm. **Figure 7.** TEM section showing Golgi dictyosome adjacent to basal bodies. The *cis* face of the Golgi is nearer the basal bodies, while the *trans* face is nearer the nucleus. The pairing of basal bodies 2 and 3 is evident. The transition region of basal body 2 is visible (arrow), as are portions of the anterior root with its associated secondary cytoskeletal microtubules, and the right ventral root. Strain 50562. Scale bar = 250 nm. **Figure 8.** Presumptive hydrogenosome. Strain 50598. Scale bar = 250 nm. **Figures 9–11.** Cross sections of the posterior flagellum, viewed tip-to-base and ventral side up. Fig. 9. Section at about the midregion of the vane-bearing section (see Figs. 2, 5), showing fullest development of the dorsal and ventral vanes. Strain 50562. Scale bar = 250 nm. **Figure 10.** Section near the flagellar insertion, showing the origin of the ventral vane and its association with a single axonemal doublet. Strain 50598. Scale bar = 250 nm. **Figure 11.** Section slightly posterior to that of Figure 10, showing the continued association of the ventral vane with one axonemal doublet and the diffuse origin of the dorsal vane. Strain 50598. Scale bar = 250 nm. **Figure 12.** Longitudinal section of the posterior flagellum, showing the striations present near the margin of the ventral vane. Strain 50598. Scale bar = 250 nm. **Figure 13.** Cross section of the flagellar transition region, showing doublet microtubules in the basal body and the central axosome into which the central microtubules of the flagellar axoneme are inserted. Strain 50562. Scale bar = 100 nm.

happened with fixed cells (Figs. 2, 5). The other two flagella projected laterally, one to the left, the other to the right.

The two strains were slightly different in size. Strain ATCC 50598 measured 11–17 μm in length and 7–13 μm in width when viewed from the side (mean 13.5 μm long, 9 μm wide, n = 25). Strain ATCC 50562 was somewhat smaller, at 9–15 μm long and 5-10 μm wide (mean 10.7 μm long, 6.5 μm wide, n = 25). Only this strain produced cyst-like structures, discussed below. No other measurable differences were seen in the light or electron microscopical features of the cells in these two strains.

The single nucleus was located in the anterior third of the cell and contained a conspicuous central nucleolus (Figs. 2, 4, 6). The nucleus was surrounded by a dense network of rough endoplasmic reticulum, which extended towards the posterior end of the cell (Figs. 4, 6). A single Golgi stack (dictyosome) was located just posterior and to the left of the basal bodies (Figs. 4, 7). The *cis* face of the dictyosome was oriented towards the basal bodies, the *trans* face towards the nucleus (Fig. 7). BODIPY-ceramide accumulation in Golgi and endoplasmic reticulum (Fig. 4) was also observed in *Reclinomonas americana* and the positive control *Trichomonas vaginalis*, but not in *T. pyriformis* cells incubated without BODIPY-ceramide, in the negative control *Vahlkampfia lobospinosa*, or in the endomembrane-lacking species *Chilomastix cuspidata* and *Retortamonas* sp. (results not shown).

Mitochondria, extrusomes and contractile vacuoles were not observed. Rod-shaped structures, presumed to represent hydrogenosomes, 0.5–1.0 μm in length and bounded by a double membrane, were dispersed throughout the cell (Figs. 6, 8).

Flagellar and cellular surfaces lacked prominent coverings. All but the posterior flagellum, with its two prominent vanes (Figs. 1, 2, 5, 9), also lacked significant inclusions apart from the standard 9 + 2 axoneme. At its origin, the ventral vane on the posterior flagellum was associated with a single axonemal doublet (Fig. 10), while the dorsal vane, initiated slightly distal to its counterpart, was not clearly associated with any component of the axoneme (Fig. 11). Both vanes had a paracrystalline substructure (Figs. 12, 19).

The kinetid consisted of four basal bodies, four microtubular roots, secondary cytoskeletal microtubules emanating from the anterior root, and various fibers associated with the basal bodies and roots.

Basal bodies were characterized by transition regions slightly recessed from the plane of the plasmalemma (Figs. 7, 20–21, 29). A central axosome was present in the transition region, into which the central doublet microtubules of the axoneme were inserted (Figs. 13, 20–21, 29). C tubules were lacking from the basal body in the vicinity of the transition region (Fig. 13).

The arrangement of the basal bodies was asymmetrical (Figs. 14–21). Basal bodies 1 and 4 formed a cross-shaped pair, with basal body 4 projecting to the left side of the cell (Figs. 14–17). Basal bodies 2 and 3 formed an L-shaped pair, anchored in fibrous material posterior to the proximal end of basal body 1 (Figs. 7, 21), with basal body 3 projecting to the right. Basal bodies 1 and 2 also formed an L-shaped pair, but with the proximal end of basal body 1 approaching the midregion, not the proximal end, of basal body 2 (Figs. 17–20).

A single microtubular root, the anterior root, emanated from the anterior basal body. It arose from the basal body's anterior surface near its proximal end (Fig. 21). It extended along the left side of the cell, initially arcing anteriorly but eventually passing posteriorly, parallel to the left ventral root (Figs. 18–21). It contained three or four microtubules (Fig. 22) and was associated through most of its length with secondary cytoskeletal microtubules that radiated from it and along the dorsal surface of the cell (Figs. 7, 19–21, 29).

Three microtubular roots arose from the posterior basal body. The left ventral root arose on the dorsal surface of the posterior basal body, just proximal to the transition region (Figs. 15–17). At its origin, four microtubules were present in the root (Fig. 23, 28), but distally the number increased by addition of ca. 10 microtubules to the left side of the root (Figs. 24–26). At a point posterior to the emergence of the posterior flagellum, the leftmost microtubules entered into a spur, or epipodium (Figs. 20–21). The remaining microtubules were limited to a narrow zone along the left boundary of the ventral groove (Figs. 3, 27). Up to the point of divergence of the epipodium, the root microtubules were subtended by short, sparse lamellae (Figs. 24–26). An unstriated fiber, the C fiber, was also present proximal to (Fig. 18–21, 24–26), but not distal to (Fig. 27), the epipodium.

An intermediate root originated dorsal to the posterior basal body (Fig. 28). The single microtubule of this root extended posteriorly, eventually becoming associated with the rightmost microtubules of the left ventral root (Fig. 24–27).

The right ventral root arose on the right side of the basal body near its proximal end (Fig. 19–21). At its proximal end, the root consisted of a small number of microtubules (Fig. 29), but additional microtubules were added distally to the right side of the

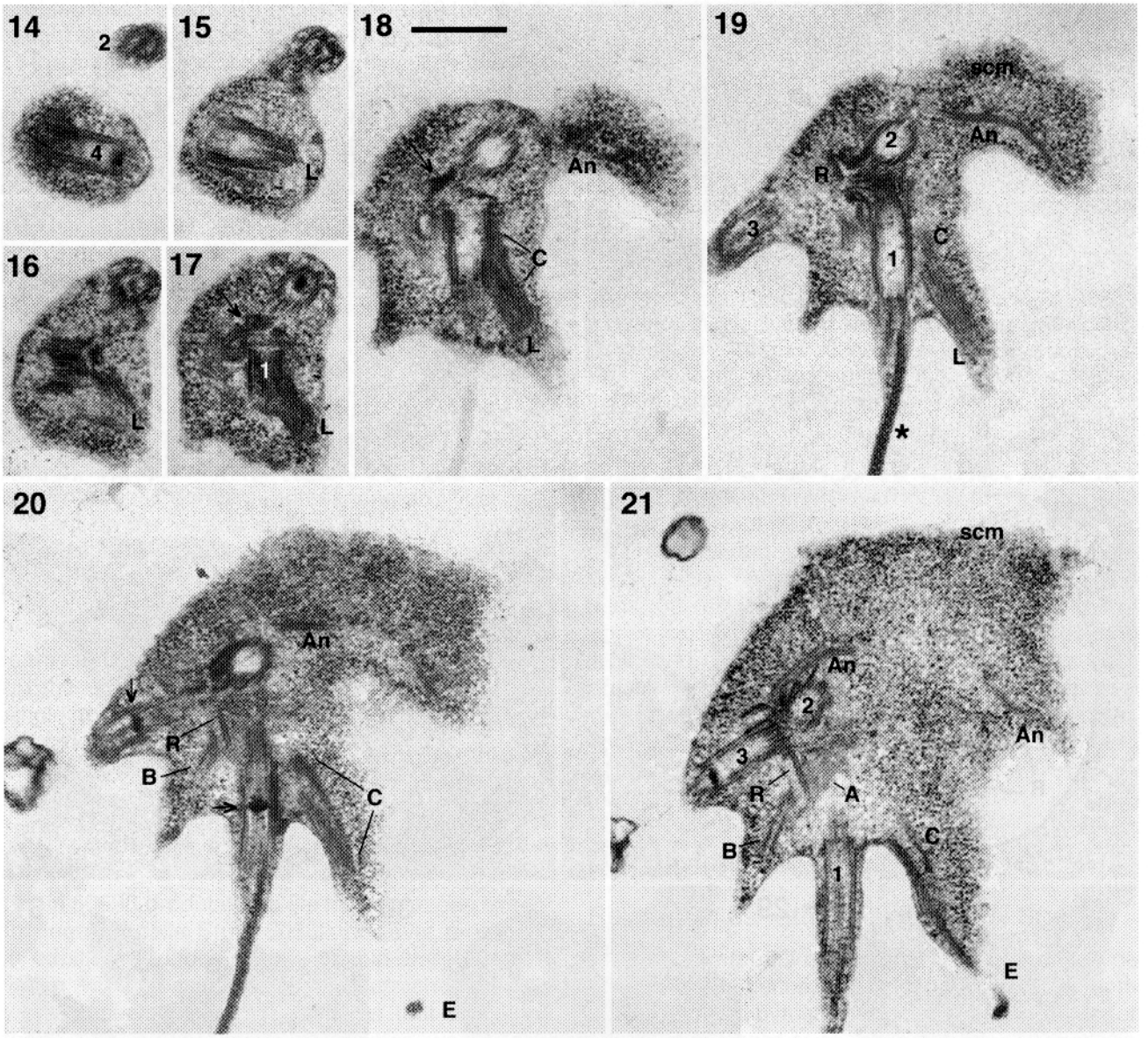


**Figures 14–21.** Serial sections through the kinetid of *Trimastix pyriformis*, viewed from the anterior end of the cell, ventral side down. Strain 50598. Scale bar (Fig. 18) = 500 nm. **Figure 14.** Anteriormost section, with basal body 4 and the flagellum arising from basal body 2. **Figure 15.** Proximal microtubules of the left ventral root. **Figure 16.** Proximal ends of the left ventral root and basal body 4, and the distal end of basal body 2. **Figure 17.** Proximal end of basal body 1 and its relationship to the left ventral root. Fibrous material (arrow) lies in the junction of basal bodies 1, 2 and 4. **Figure 18.** Origin of the C fiber subtending the left ventral root. A segment of the anterior root is visible. Fibrous material (arrow) extends towards basal body 2. **Figure 19.** Origin of the right ventral root. Secondary cytoskeletal microtubules emanate from the vicinity of the anterior root. Striations are visible in the ventral vane of the posterior flagellum (asterisk). Fibrous material lies between the basal bodies. **Figure 20.** Origin of the B fiber associated with the right ventral root. The transition regions of basal bodies 1 and 3 are indicated (arrows), as are segments of the anterior root and the left ventral root with its associated C fiber and epipodium. **Figure 21.** Posteriormost section. Junction of basal bodies 2 and 3, the origin and distal continuation of the anterior root, the left ventral root with associated C fiber and epipodium, and the right ventral root with associated B fiber.

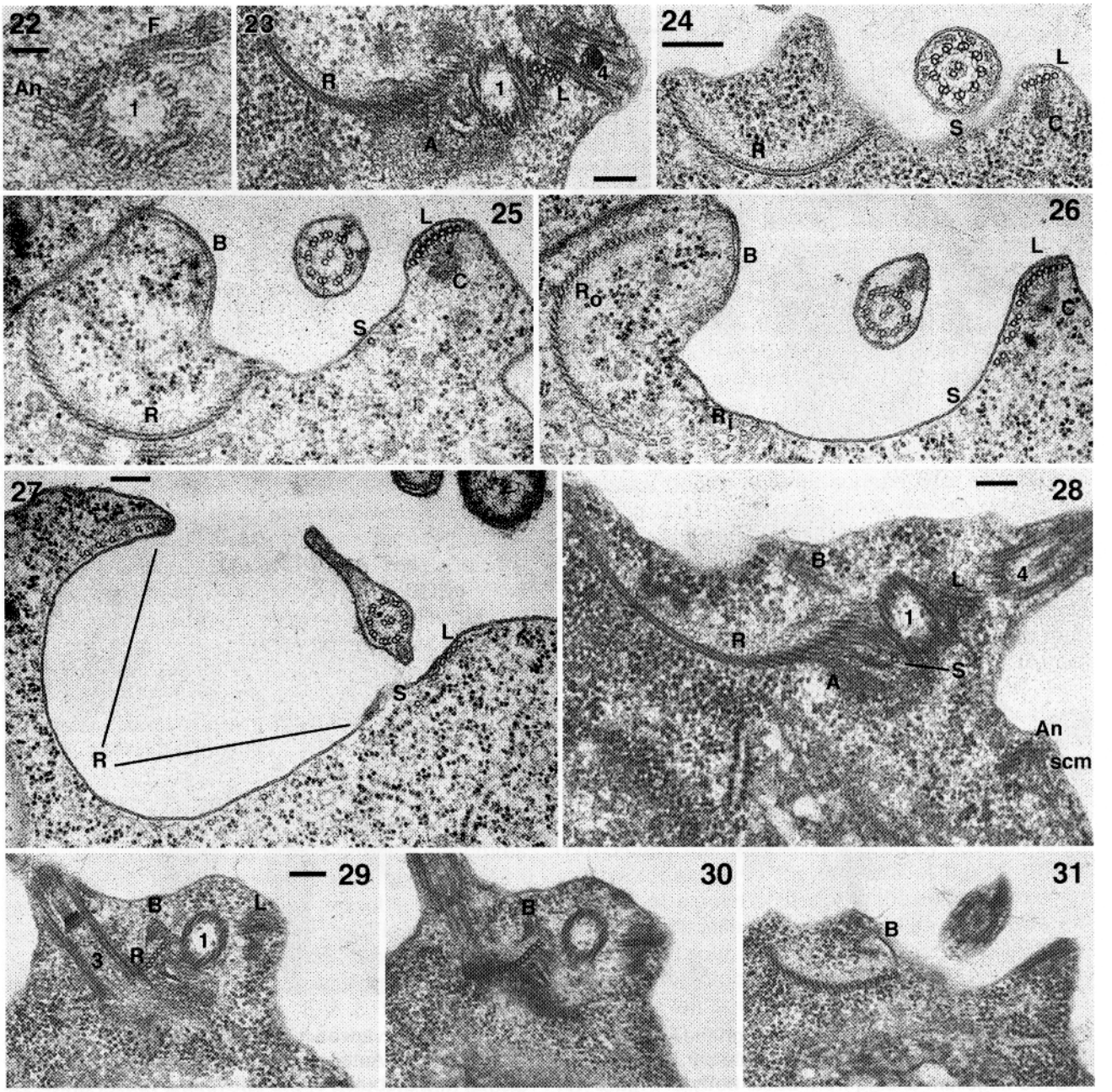


**Figures 22–31.** Microtubular root architecture of *Trimastix pyriformis*. **Figure 22.** Proximal end of the anterior root, arising from near basal body 2. The band connecting basal bodies 2 and 3 is also visible. Strain 50562. Scale bar = 100 nm. **Figure 23.** Origin of the left ventral root, showing four microtubules and small fibers under each microtubule. Fibrous material (A fiber) extends from basal body 1 to subtend the right ventral root. Strain 50598. Scale bar = 250 nm. Figures 24–27. Strain 50562. Figures 24–26 are from a series of sections from a single cell, scale bar (Fig. 24) = 250 nm. **Figure 24.** Near the level of the transition region of basal body 1, the left ventral root contains five microtubules, each with small fibers, and is subtended by the C fiber. The intermediate singlet root lies in the ventral groove, while the right root is off to the side. Clear zone ventral to the right root represents the I fiber. **Figure 25.** The left root contains nine tubules, the new ones added to the inside of the root. **Figure 26.** The left root contains 15 tubules, with the innermost six slightly dissociated from the remainder. Six microtubules are dissociated from the right root, forming an indistinct inner subunit. **Figure 27.** Near the midpoint of the cell, the left root, its 7-8 microtubules lacking small fibers, form a group near the left margin of the ventral groove, with the intermediate singlet microtubule nearby. Microtubules of the right root line the remainder of the ventral groove. Left root micro-

root, so that it eventually contained ca. 30 tubules in a tight spline (Figs. 24–25, 30–31). At a point distal to the emergence of the posterior flagellum, the leftmost microtubules separated from the remainder, forming an indistinct inner subunit of the root (Fig. 26). These inner subunit microtubules eventually formed a sparse lining for the ventral groove (Fig. 27). The rightmost microtubules, forming the outer subunit of the root, defined the protruding margin of the ventral groove (Figs. 3, 27).

Fibrous material, the A fiber, was associated with the dorsal surface of the right root at its proximal end, originating near the proximal ends of basal bodies 1 and 4 (Figs. 21, 23, 28, 30). Another electron-dense fiber, the B fiber, originating from around the midregion of basal body 1(Figs. 20–21, 29–30), extended posteriorly ventral to the right root and along the plasmalemma (Figs. 24–26, 31). A less electron-dense domain, representing an I fiber, was present on the ventral surface of the right root for much of its length (Figs. 24–26, 28, 31). Fibrous material was found at the right margin of the root near the posterior end of the ventral groove (Figs. 3, 27).

The microtubular roots, with the exception of the leftmost microtubules of the left ventral root making up the epipodium and, possibly, the intermediate singlet root, reunited at the posterior end of the ventral groove (Fig. 3).

A diagrammatic reconstruction of the kinetid appears in Fig. 41.

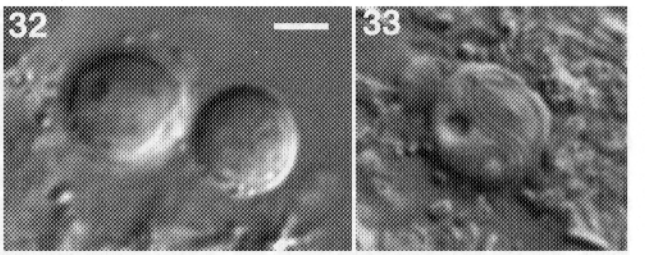


**Figures 32–33.** Cysts of *Trimastix pyriformis* strain 50598. Differential interference contrast. Scale bar = 5 μm. **Figure 32.** Habit shot of two cysts, showing spherical shape and lack of ornamentation. **Figure 33.** Image showing two of four flagellar axonemes conserved within the cyst, emanating from a basal body complex near the upper margin of the cyst.

### Cysts

Strain 50598 produced no life history stages except for flagellate cells. Strain 50562, however, produced, in addition, rounded cells with thin walls (Fig. 32) within which basal bodies and attached flagella were preserved (Fig. 33). Cultures that contained these cells but not active flagellates would yield flagellates if stored at 20–25 °C for no more than six weeks before transfer into fresh medium.

### Cell Division

Some stages of cell division were observed in flagellate cells. Flagella were retained throughout division (Figs. 34,40). Preprophase development was signalled by replication of basal bodies and the appearance of non-root microtubules near the basal bodies (Fig. 38). Chromosomes formed a distinct metaphase plate, separating into two during anaphase (Figs. 36–40). No nucleoli were detected at metaphase or anaphase. By metaphase, kinetids had replicated, and microtubular root templates were present (Figs. 36, 39–40). The metaphase spindle was open, and was composed of two half spindles emanating from the basal body complexes situated at the spindle poles (Figs. 39–40).

## Discussion

### Relationships with Other *Trimastix* Species

*Trimastix pyriformis* differs from *T. marina*, the type species of the genus, which is marine and has both a differentiated cytostome and a thickened anterior flagellum (Bernard et al. 1999; Kent 1880; Simpson et al. unpublished). The ultrastructural features of *T. marina* are under investigation (Simpson et al. unpublished). *Trimastix pyriformis* also differs from *T. inaequalis*, in which flagella 3 and 4 are of unequal length (Bernard et al. 1999).

*Trimastix pyriformis* is most similar to *T. convexa* in its external morphology, the position and structure of the Golgi stack, the position and structure of

tubules in the epipodium are not shown. A fiber appears at the right margin of the ventral groove. Scale bar = 250 nm. **Figure 28.** Origin of the intermediate singlet root. The left, right and anterior roots are also visible. Strain 50598. Scale bar = 250 nm. Figures 29–31. Views of the right ventral root, from a single cell, serial sections. Strain 50598, scale bar (Fig. 29) = 250 nm. **Figure 29.** Origin of the root, showing six microtubules and associated B fiber. **Figure 30.** Adjacent section, the root has 9 microtubules. **Figure 31.** The root has ca. 30 microtubules.

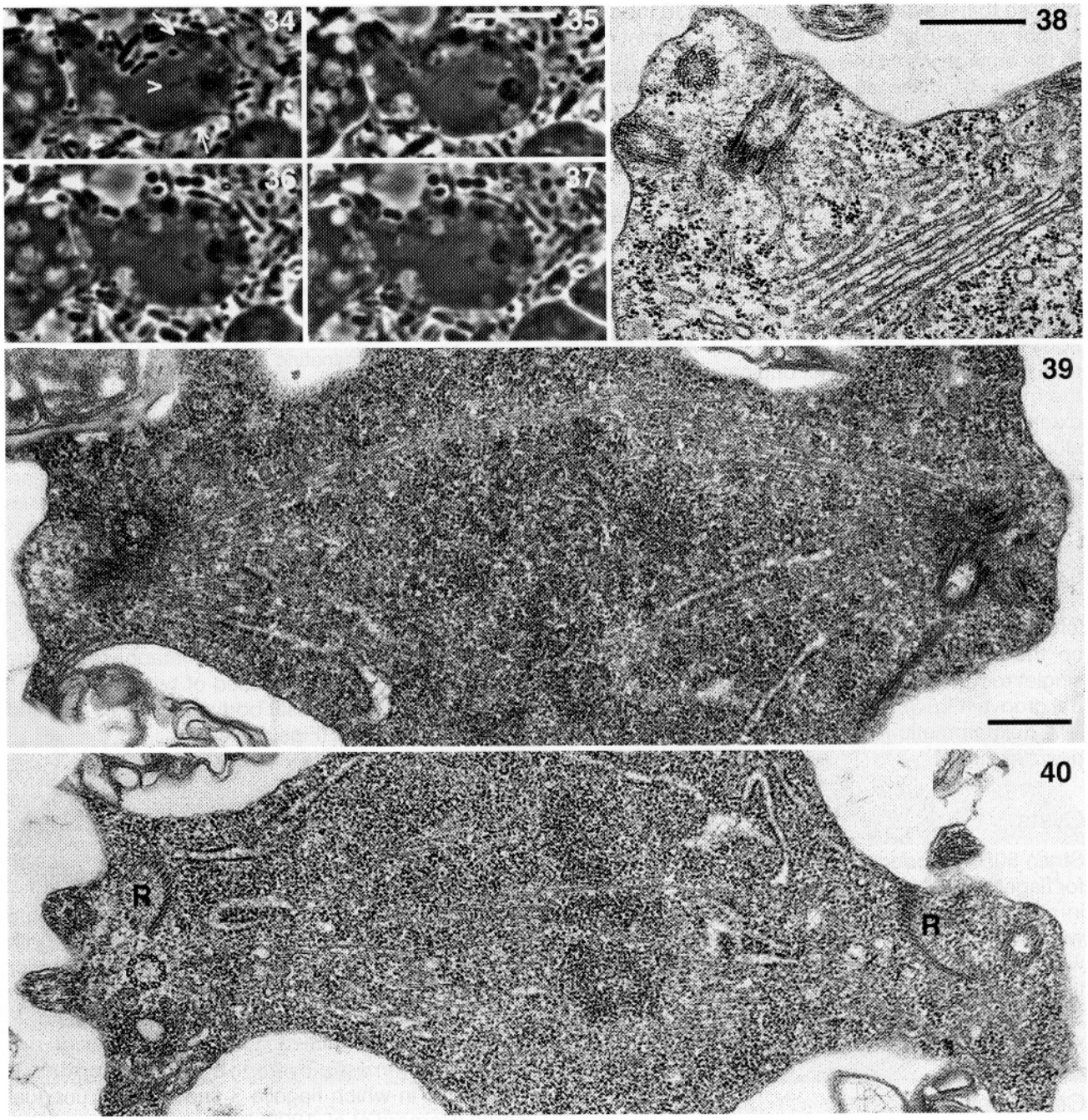


**Figures 34–40.** Dividing cells of *Trimastix pyriformis*. Figures 34–37. Phase contrast light micrographs of a single live cell in mitosis. Strain 50598. Scale bar (Fig. 35) = 5 μm. **Figure 34.**Tangential optical section of the cell at metaphase, showing positions of spindle poles with two flagella at each pole (arrows). Arrowhead shows position of metaphase plate. **Figure 35.** Medial optical section of same cell at same time, showing metaphase plate. **Figure 36.** Early anaphase. **Figure 37.** Late anaphase. Approximately 20 seconds have elapsed between Figs. 35 and 37. **Figure 38.** TEM of kinetid region in preprophase cell, with newly-formed basal bodies and non-root microtubules arising from a mature basal body. Strain 50562. Scale bar = 250 nm. Figs. 39–40. Two sections of a metaphase plate. Strain 50598. Scale bar (Fig. 39) = 500 nm. **Figure 39.** A more median view of the spindle. Spindle microtubules extend from the chromosomal plate to the poles, focusing on the basal body complexes. Interzonal microtubules, nuclear envelope and nucleolar material are absent. **Figure 40.** A more tangential view. Three (of four) basal bodies are visible at one pole, and templates of the right ventral root are visible at both poles.

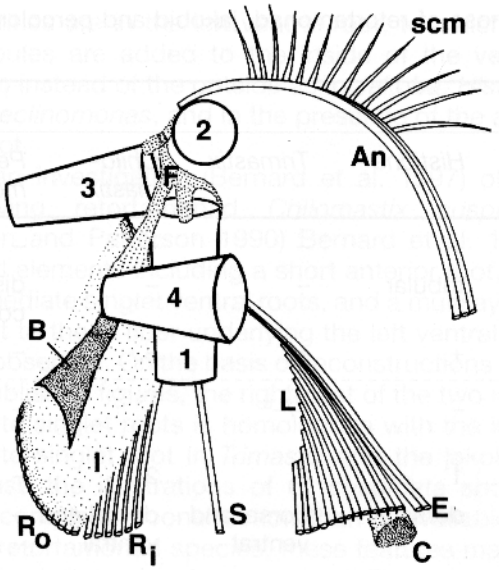


**Figure 41.** Interpretive diagram of the *Trimastix pyriformis* kinetid. Not to scale.

the posterior flagellum, the composition and orientation of the major kinetid components, and the overall architecture of the ventral groove complex. However, the cells of *T. pyriformis* are smaller than those of *T. convexa* and are close to the size ranges for *T. pyriformis* reported by Klebs (1892, as *Tetramitus pyriformis*) and subsequent workers (Bernard et al. 1999; Calaway and Lackey 1962 ). Also, the anterior root has two microtubules in *T. convexa* instead of three or four as in *T. pyriformis*, and the winglike fibers associated with the distal end of the left ventral root in *T. convexa* are absent from *T. pyriformis*.

On this evidence, *T. convexa* and *T. pyriformis* are here retained as separate species, not combined under *T. pyriformis* as in Bernard et al. (1999). These two species and *T. inaequalis*, though, may be members of a species complex. Determination of the species boundaries in this putative complex, if there are any, requires examination of additional samples and integrated analysis of these samples with, at least, microscopical and molecular methods.

## Relationships of *Trimastix pyriformis* with Other Protists

Brugerolle and Patterson (1997) compared the genus *Trimastix* with retortamonads, with other "archezoan" (sensu Cavalier-Smith 1987, 1993) protists, and with heteroloboseans. They found that, of all of these protists, retortamonads were the most similar to *Trimastix*. The similarities included the architecture of the ventral groove, the presence and structure of the vanes on the posterior flagellum, and the arrangement of the basal bodies and microtubular roots in the kinetid.

To this list of features may be added those of the mitotic spindle as seen here in *T. pyriformis*. The organization of the microtubules into two half-spindles focused on the replicated basal body complexes corresponds well with what has been observed in the retortamonad genera *Chilomastix* and *Retortamonas* (Brugerolle 1973, 1977; Brugerolle and Mignot 1990). One difference is the absence of nuclear membrane and nucleolar material from *Trimastix* mitotic figures.

As noted by Brugerolle and Patterson (1997) and confirmed here, *Trimastix* differs from retortamonads by possessing hydrogenosome-like structures. The presumptive hydrogenosomes in *T. pyriformis* are similar in size and distribution to those in *T. convexa*. Differences in electron density between the presumptive hydrogenosomes of *T. pyriformis* and *T. convexa* might be due to different fixation protocols.

*Trimastix* also differs from retortamonads by possesssing endoplasmic reticulum and Golgi that are visible by standard transmission electron microscopy and by accumulation of fluorescently-labelled membrane-specific lipids (Pagano et al. 1991).

Brugerolle and Patterson (1997) did not compare *Trimastix* with the jakobid flagellates (genera *Jakoba, Histiona, Reclinomonas, Malawimonas*; O'Kelly 1993, 1997; O'Kelly and Nerad 1999). Several parallels exist among these genera (Table 1). In both *Trimastix* and the jakobids, the Golgi dictyosome is near the flagellar insertion, and the *trans* face appears to be oriented towards the nucleus. In both, there are three longitudinally-oriented ventral roots that define a conspicuous ventral groove. In both, the right root produces no gullet-associated loop structure as in retortamonads, but instead forms a splinar array that eventually becomes associated with the right margin and floor of the ventral groove. In both, the outer microtubules of the left ventral root separate from the others, forming either an epipodium or a flange near the proximal end of the root. In both, the flagellar roots are associated with the A, B, C and I fibers first identified in *Jakoba libera* (Patterson 1990) and *Reclinomonas americana* (O'Kelly 1997). In both, the mitotic spindle is composed of two half-spindles, each focused on a basal body complex (O'Kelly 1993 and unpublished).

Of the known jakobids, *Malawimonas jakobiformis* (Malawimonadidae; O'Kelly and Nerad 1999) most closely resembles *T. pyriformis*. The greatest

**Table 1.** Ultrastructural features of *Trimastix* compared with those of retortamonad, jakobid and percolomonad flagellates.

| Feature | Taxon | | | | | | |
|---|---|---|---|---|---|---|---|
| | *Malawimonas* | *Jakoba* | *Reclinomonas* | *Histiona* | *Trimastix* | *Chilomastix* | *Percolomonas* |
| Extrusomes | + | + | + | + | – | – | – |
| mitochondrial cristae | discoidal | plate/tubular[a] | tubular | tubular | – | – | discoidal |
| Golgi | + | + | + | + | + | – | – |
| Differentiated cytostome/cytopharynx | – | – | – | – | +/–[b] | + | – |
| Posterior Flagellar Vane | 1–2[c] | 1 | 1 | 1 | 2 | 2 | – |
| Origin of Vane | (dorsal and) ventral | dorsal | dorsal | dorsal | dorsal and ventral | dorsal and ventral | – – |
| Distal Fiber (between basal bodies 1 and 2) | + | – | + | + | – | – | – |
| L + R roots define floor of ventral groove | mostly R | mostly L | mostly L | mostly L | mostly R[d] | equal[e] | ? |
| L + R roots parallel to cell long axis | + | + | + | + | + | + | – |
| "Ribbed" Root | + | – | – | – | + | + rd | – |
| R root: A fiber | + | + | + | + | + rd | – | + |
| R root: B fiber | + rd | + | + | + rd | + | – | ? |
| R root: I fiber | + | + | + | + | + | + | + |
| L root: C fiber | + rd | + | + | + | + | + | ? |
| L root: MLS | – | + | + | + | + rd | + | ? |
| "Epipodium" | + | – | + | + | + | – | – |
| MTs added to side of L root | in | out | out | out | in | out | ? |
| S root | + | +[f] | + | + | + | + | ? |

+, present; rd, present but smaller or less elaborate in structure than in other species; –, absent; ?, character state unknown.

[a] irregularly platelike in *J. libera* but tubular in a second species, as yet undescribed (O'Kelly and Nerad, unpublished).

[b] identified in *T. marina* by Bernard et al. (1999), but absent from the other three species in the genus (Bernard et al. 1999; Brugerolle and Patterson 1997; this study).

[c] one ventral vane in *Malawimonas jakobiformis*, two vanes in a second species, as yet undescribed (O'Kelly and Nerad, unpublished).

[d] unlike jakobid and retortamonad species, the ventral roots in *Trimastix* remain associated with the margins of the ventral groove, few are found in the floor of the groove (this study).

[e] most of the microtubules of the right root are associated with the gullet, those microtubules in the non-gullet portions of the ventral groove are about equally contributed from the left and right roots (Bernard et al. 1997; Brugerolle 1973).

[f] not yet convincingly demonstrated in *J. libera*, but present in the new species (note a).

References: *Malawimonas*, O'Kelly and Nerad 1999 and unpublished; *Reclinomonas*, O'Kelly 1993, 1997; *Jakoba*, O'Kelly 1997; O'Kelly and Nerad unpublished; Patterson 1990; *Histiona*, Mylnikov 1989; O'Kelly and Nerad unpublished; *Trimastix*, Bernard et al. 1999; Brugerolle and Patterson 1997; this study; *Chilomastix*, Bernard et al. 1997; Brugerolle 1973; *Percolomonas*, Fenchel and Patterson 1986; O'Kelly unpublished.

similarities are in the left ventral root, to which microtubules are added to the inside of the ventral groove instead of the outside as in *Jakoba, Histiona* and *Reclinomonas*, and in the presence of the anterior root.

In an investigation (Bernard et al. 1997) of the free-living retortamonad *Chilomastix cuspidata* (Larsen and Patterson 1990) Bernard et al. 1997, kinetid elements including a short anterior root, two intermediate singlet ventral roots, and a multilayered aspect to the C fiber underlying the left ventral root were observed. On the basis of reconstructions from the published figures, the rightmost of the two intermediate singlet roots is homologous with the intermediate singlet root in *Trimastix* and the jakobids. Because the illustrations of *C. cuspidata* show a more complete reconstruction than is available for other retortamonad species, these features may be common but previously overlooked. These observations are consistent with a close phylogenetic relationship among the jakobids, the retortamonads, and *Trimastix* (Table 1).

Most jakobids differ from retortamonad and *Trimastix* species by having only one vane on the posterior flagellum (Table 1). The single vane in *Malawimonas jakobiformis* arises on the ventral surface of the flagellum and is associated with a specific region of the axoneme (O'Kelly and Nerad 1999), like the ventral vane in *T. pyriformis*. The single vane in *Reclinomonas, Histiona* and *Jakoba* arises on the dorsal flagellar surface and is not visibly associated with any particular axonemal component (Mylnikov 1989; O'Kelly 1997; Patterson 1990), like the dorsal vane in *T. pyriformis*. If the jakobids had a *Trimastix*-like ancestor, then differential loss of one or the other of the two vanes would account for the present distribution of this feature.

Brugerolle and Patterson (1997) argued that *Trimastix* could not be assigned to the trichomonads (Grassé 1952). Basal bodies are arranged differently in the two groups, *Trimastix* species lack kinetid elements diagnostic for trichomonads (costal and parabasal fibers, axostyle) and trichomonads lack a ventral groove. *Trimastix* species also lack the trichomonad undulating membrane and associated fibers, as well as the parabasal fiber linking the basal bodies to the Golgi stack. The present work confirms their observations and supports their argument. In addition, as shown here, *T. pyriformis* lacks the highly-organized interzonal mitotic spindle that is characteristic for trichomonads (Brugerolle 1975; Juliano et al. 1986). The placement of *Trimastix* with trichomonads in the Trichozoa, rather than with retortamonads in the Metamonada, by Cavalier-Smith (1996–97, 1998) was justified by the presumed postendosymbiotic shared gain of Golgi and hydrogenosomes by *Trimastix* and trichomonads. This justification seems inadequate since the interphase and mitotic features of *Trimastix* are more like those of retortamonads and jakobids than trichomonads. Moreover, confirmation from biochemical and molecular studies that the *Trimastix* structures are hydrogenosomes has not yet been achieved.

## *Trimastix* and the Early Evolution of Eukaryotes

Jakobid flagellates also differ from retortamonads and *Trimastix* by having mitochondria. These mitochondria have the most eubacterial-like genomes of any eukaryotes examined to date (Gray et al. 1998, 1999; Lang et al. 1997, 1998). Initially, the ultrastructural similarities between jakobids and retortamonads suggested that the jakobids might be among the most ancient mitochondrial eukaryotes (O'Kelly 1993), an hypothesis seemingly supported by the mitochondrial genome findings and by the rediscovery of *Trimastix* species with ultrastructural features resembling both groups.

However, other researchers have found mitochondrial genes in members of the diplomonad (Hashimoto et al. 1998; Keeling and Doolittle 1997; Roger et al. 1998) and other "archezoan" lineages (Germot et al. 1996; Horner et al. 1996; Keeling and Doolittle 1997; Roger et al. 1996). It is now thought that the "archezoan" protists lost mitochondria rather than having never had them, and that mitochondria evolved very early in eukaryote evolution (Gray et al. 1999; Sogin 1997; Sogin and Silberman 1998). In such a scenario, *Trimastix* and the jakobid, retortamonad, and diplomonad protists may still retain a prominent place. A retortamonad-like mitochondriate ancestor may have given rise to the retortamonad/diplomonad and *Trimastix* lineages by loss of mitochondria, and to the jakobid lineages by reduction in size and number of expressed flagella. It would be worthwhile to probe the nuclear genomes of these protists for mitochondrial genes, and to investigate the function of the hydrogenosome-like organelles in *Trimastix* species.

The presence of endoplasmic reticulum and Golgi in *Trimastix* may also provide new information on the evolution of endomembranes in eukaryotes. A key element of the Archezoa hypothesis (Cavalier-Smith 1987) is that endomembrane systems, in particular the Golgi apparatus, evolved only after the endosymbiotic acquisition of mitochondria, and did not appear in some of the most basally-derived protist lineages, such as the Heterolobosea, even after mitochondrial acquisition (Cavalier-Smith 1993, 1996–97).

Evidence from the diplomonad genus *Giardia*, however, indicates that Golgi and endoplasmic reticulum structure and function are not lost but modified (Luján et al. 1995; Soltys et al. 1996), presumably in response to changed cellular demands on the endomembrane system (Becker and Melkonian 1996; Gillin et al. 1996). If *Trimastix* represents an ancient form of eukaryote, then all extant eukaryotes studied to date are descended from an ancestor with "canonical" endomembranes (those readily seen in "standard" chemically-fixed, resin-embedded and sectioned transmission electron microscopy preparations). These endomembrane systems would then have been lost or (more probably) modified in particular lineages, including the retortamonads, diplomonads and heteroloboseans.

## Methods

**Isolation and cultivation:** *Trimastix pyriformis* was isolated from a swampy area in Rock Creek Park, Rockville, Maryland, USA, on 8 November 1995 (strain ATCC 50562), and from water accumulated in an underground ventilation tunnel at Logan Airport, Boston, Massachusetts, USA, on 21 May 1996 (strain ATCC 50598). Both were freshwater habitats. Clonal isolates were prepared by single-cell isolation methods (Molina and Nerad 1991); in the case of the Rockville strain, this was after incubation of the crude sample in ATCC medium 1773 (Nerad 1993), a selective medium from which only *T. pyriformis* was recovered. One clone of each isolate was cryopreserved (Nerad and Daggett 1992; Poynter et al. 1995) and deposited in ATCC. Material for microscopic examination was reactivated from cryopreserved samples and maintained in 16 × 125 mm screw-capped glass test tubes filled with 12 mL of ATCC medium 802, bacterized with *Enterobacter aerogenes* ATCC 13048, at 15–25 °C.

**Light microscopy:** Light microscopical observations were made on live cells viewed on a Zeiss Axioskop light microscope equipped with bright-field, phase-contrast and differential interference contrast optics. Images of live motile cells were captured using an Optronics DEI-470 CCD camera and digitized using TCPro version 2.31 (Coreco). Other micrographs were made on Kodak Technical Pan 35mm film, exposed at ISO 25 and processed with Kodak Technidol developer.

**Fluorescent labelling of endomembranes:** Labelling of Golgi and endoplasmic reticulum membranes was accomplished through a procedure modified from Takizawa et al. (1993). Living cells were incubated for 10-60 min in 50 mmol *N*-[5-(5,7-dimethyl boron dipyrromethene difluoride)-1-pentanoyl]-D-*erythro*-sphingosine (BODIPY-ceramide; Molecular Probes Inc.) in culture medium, and examined on an Olympus photomicroscope equipped with confocal laser optics (Bio-Rad). Some cells were fixed in 2.5% glutaraldehyde in culture medium and washed twice in water before incubation in 50 mmol BODIPY-ceramide in water and examination as above. The jakobid *Reclinomonas americana* ATCC 50284 and the retortamonads *Retortamonas* sp. ATCC 50375 and *Chilomastix cuspidata* ATCC 50576 were also examined. A positive control was provided by the Golgi-containing trichomonad *Trichomonas vaginalis* ATCC 30001, a negative control by the Golgi-lacking heterolobosean *Vahlkampfia lobospinosa* ATCC 30298.

**Transmission electron microscopy:** Cells were fixed, serially sectioned, stained and examined using procedures slightly modified from those described in detail elsewhere (O'Kelly 1997; O'Kelly and Patterson 1996). Briefly, exponential-phase cells were fixed in a cacodylate-buffered glutaraldehyde-osmium cocktail for 15–60 min at room temperature (ca. 20 °C). Fixed cells were filtered onto cellulose acetate/nitrate wafers, washed with distilled water, enrobed in agar, dehydrated in a graded acetone series and embedded in epoxy (Epon or Spurr) resins. Blocks were trimmed by hand, serially sectioned with a diamond knife, mounted on uncoated mesh grids or formvar/carbon coated slots, stained with uranyl acetate and lead citrate, and examined with a Zeiss EM 902 transmission electron microscope operating at 80 kV.

**Terminology:** Conventions for cell components and kinetid absolute configuration follow O'Kelly (1993, 1997). It is assumed that the eldest basal body bears the posteriorly-directed, vane-bearing flagellum, as in jakobids (O'Kelly 1993 and unpublished), so this basal body is assigned the numeral "1" (Melkonian et al. 1987; Moestrup and Hori 1989).

**Internet data dissemination:** Updated summaries on the morphology, taxonomy and biology of *Trimastix* species are available from the Protist Image Data Web site (http://megasun.bch.umontreal.ca/protists/trim/).

## Acknowledgements

We are grateful to the National Science Foundation for research support to TAN (grant DBI-9401876), and to David J. Patterson, Catherine Bernard and Alastair G. B. Simpson for pre-publication information on *Trimastix marina, T. inaequalis* and Australian

isolations of *T. pyriformis* as well as on other protists referrable to this general protist assemblage.

## References


**Becker B, Melkonian M** (1996) The secretory pathway of protists: spatial and functional organization and evolution. Microbiol Rev **60**: 697–721

**Bernard C, Simpson AGB, Patterson DJ** (1997) An ultrastructural study of a free-living retortamonad, *Chilomastix cuspidata* (Larsen & Patterson, 1990) n. comb. (Retortamonadida, Protista). Europ J Protistol **33**: 254–265

**Bernard C, Simpson AGB, Patterson DJ** (1999) Some free-living flagellates (Protista) from anoxic habitats. Ophelia (in press)

**Brugerolle G** (1973) Etude ultrastructurale du trophozoite et du kyste chez le genre *Chilomastix* Alexeieff, 1910 (Zoomastigophorea, Retortamonadida Grassé, 1952). J Protozool **20**: 574–585

**Brugerolle G** (1975) Etude de la cryptopleuromitose et de morphogenèse de division chez *Trichomonas vaginalis* et chez plusieurs genres de trichomonadines primitives. Protistologica **11**: 457–468

**Brugerolle G** (1977) Ultrastructure du genre *Retortamonas* Grassi 1879 (Zoomastigophorea, Retortamonadida Wenrich 1931). Protistologica **13**: 223–240

**Brugerolle G, Mignot J-P** (1990) Phylum Zoomastigina, Class Retortamonadida. In Margulis L, Corliss JO, Melkonian M, Chapman DJ (eds) Handbook of Protoctista. Jones and Bartlett, Boston, pp. 259–265

**Brugerolle G, Patterson D** (1997) Ultrastructure of *Trimastix convexa* Hollande, an amitochondriate anaerobic flagellate with a previously undescribed organization. Europ J Protistol **33**: 121–130

**Calaway WT, Lackey JB** (1962) Waste Treatment Protozoa: Flagellata. Florida Engineering Series No. 3, Florida Engineering and Industrial Experiment Station, Gainesville, FL, 140 pp

**Cavalier-Smith T** (1987) Eukaryotes with no mitochondria. Nature **326**: 332–333

**Cavalier-Smith T** (1993) Kingdom Protozoa and its 18 phyla. Microbiol Rev **57**: 953–994

**Cavalier-Smith T** (1996/1997) Amoeboflagellates and mitochondrial cristae in eukaryote evolution: megasystematics of the new protozoan subkingdoms Eozoa and Neozoa. Arch Protistenkd **147**: 237–258

**Cavalier-Smith T** (1998) A revised six-kingdom system of life. Biol Rev Camb Philos Soc **73**: 203–266

**Fenchel T, Patterson DJ** (1986) *Percolomonas cosmopolitus* (Ruinen) n. gen., a new type of filter feeding flagellate from marine plankton. J Mar Biol Assn UK **66**: 465–482

**Germot A, Phillipe H, Le Guyader H** (1996) Presence of a mitochondrial-type 70-kDa heat shock protein in *Trichomonas vaginalis* suggests a very early mitochondrial endosymbiosis in eukaryotes. Proc Natl Acad Sci USA **93**: 14614–14617

**Gillin FD, Reiner DS, McCaffery JM.** (1996) Cell biology of the primitive eukaryote *Giardia lamblia*. Annu Rev Microbiol **50**: 679–705

**Grassé PP** (1952) Ordre des Trichomonadines. In Grassé PP (ed) Traité de Zoologie, vol. 1, fasc. 1. Masson, Paris, p 704

**Gray MW, Burger G, Lang BF** (1999) Mitochondrial evolution. Science **283:** 1476–1481

**Gray MW, Lang BF, Cedergren R, Golding GB, Lemieux C, Sankoff D, Turmel M, Brossard N, Delage E, Littlejohn TG, Plante I, Rioux P, Saint-Louis D, Zhu Y, Burger G** (1998) Genome structure and gene content in protist mitochondrial DNAs. Nucleic Acids Res **26**: 865–878

**Hashimoto T, Sanchez LB, Shirakura T, Müller M, Hasegawa M** (1998) Secondary absence of mitochondria in *Giardia lamblia* and *Trichomonas vaginalis* revealed by valyl-tRNA synthetase phylogeny. Proc Natl Acad Sci USA 95: 6860–6865

**Horner DS, Hirt RP, Kilvington S, Lloyd D, Embley TM** (1996) Molecular data suggest an early acquisition of the mitochondrion endosymbiont. Proc Roy Soc London B **263**: 1053–1059

**Juliano C, Rubino S, Zicconi D, Cappuccinelli P** (1986) An immunofluorescent study of the microtubule organization in *Trichomonas vaginalis* using antitubulin antibodies. J Protozool **33**: 56–59

**Keeling PJ, Doolittle WF** (1997) Evidence that eukaryotic triosephosphate isomerase is of alpha-proteobacterial origin. Proc Natl Acad Sci USA **94**: 1270–1275

**Kent WS** (1880) Manual of the Infusoria: flagellate, ciliate and tentaculiferous Protozoa, British and foreign, vol. 1, pp. 310–315.

**Klebs G** (1892) Flagellatenstudien. Zeit wiss Zool **55**: 265–445

**Lang BF, O'Kelly CJ, Burger G** (1998) Mitochondrial genomics in protists, an approach to probe eukaryotic evolution. Protist **149**: 313–322

**Lang BF, Burger G, O'Kelly CJ, Cedergren R, Golding GB, Lemieux C, Sankoff D, Turmel M, Gray MW** (1997) An ancestral mitochondrial DNA resembling a eubacterial genome in miniature. Nature **387**: 493–497

**Luján HD, Marotta A, Mowatt MR, Sciaky N, Lippincott-Schwartz J, Nash TE** (1995) Developmental induction of Golgi structure and function in the primitive eukaryote *Giardia lamblia*. J Biol Chem **270**: 4612–4618

**Melkonian M, Reize IB, Preisig HR** (1987) Maturation of a flagellum/basal body requires more than one cell cycle in algal flagellates: studies on *Nephroselmis oli-*

*vacea* (Prasinophyceae). In Wiessner W, Robinson DG, Starr RC (eds) Algal Development (Molecular and Cellular Aspects). Springer-Verlag, Berlin, pp. 102–134

**Moestrup Ø, Hori T** (1989) Ultrastructure of the flagellar apparatus in *Pyramimonas octopus* (Prasinophyceae). II. Flagellar roots, connecting fibres and numbering of individual flagella in green algae. Protoplasma **148**: 41–58

**Molina FI, Nerad TA** (1991) Ultrastructure of *Amastigomonas bermudensis* ATCC 50234 sp. nov., a new heterotrophic marine flagellate. Europ J Protistol **27**: 386–396

**Mylnikov AP** (1989) [The fine structure and systematic position of *Histiona aroides* (Bicoecales)]. Bot Zhur **74**: 184–189 [in Russian].

**Nerad TA, ed** (1993) American Type Culture Collection Catalogue of Protists, 18th edn. American Type Culture Collection, Rockville, Maryland

**Nerad TA, Daggett P-M** (1992) Cryopreservation of diplomonads other than *Giardia*. In Lee JJ, Soldo AT (eds) Protocols in Protozoology, vol. 1. Society of Protozoologists, Lawrence, Kansas, pp. A70.1–A70.2

**O'Kelly CJ** (1993) The jakobid flagellates: structural features of *Jakoba*, *Reclinomonas* and *Histiona* and implications for the early diversification of eukaryotes. J Euk Microbiol **40**: 627–636

**O'Kelly CJ** (1997) Ultrastructure of trophozoites, zoospores and cysts of *Reclinomonas americana* Flavin & Nerad, 1993 (Protista *incertae sedis*: Histionidae). Europ J Protistol **33**: 337–348

**O'Kelly CJ, Nerad TA** (1999) *Malawimonas jakobiformis* n. g., n. sp. (Malawimonadidae n. fam.): a *Jakoba*-like flagellate with discoidal mitochondrial cristae. J Euk Microbiol **46**: 522–531

**O'Kelly CJ, Patterson DJ** (1996) The flagellar apparatus of *Cafeteria roenbergensis* Fenchel & Patterson, 1988 (Bicosoecales = Bicosoecida). Europ J Protistol **32**:216–226.

**Pagano RE, Martin OC, Kang HC, Haugland RP** (1991) A novel fluorescent ceramide analogue for studying membrane traffic in animal cells: accumulation at the Golgi apparatus results in altered spectral properties of the sphingolipid precursor. J Cell Biol **113**: 1267–1279

**Patterson DJ** (1990) *Jakoba libera* (Ruinen, 1938), a heterotrophic flagellate from deep oceanic sediments. J Mar Biol Assn UK **70**: 381–393

**Poynton SL, Fraser W, Francis-Floyd R, Rutledge P, Reed P, Nerad TA** (1995) *Spironucleus vortens* n. sp. from the freshwater angelfish *Pterophyllum scalare*: morphology and culture. J Euk Microbiol **42**: 731–742

**Roger AJ, Clark CG, Doolittle WF** (1996) A possible mitochondrial gene in the early-branching amitochondriate protist *Trichomonas vaginalis*. Proc Natl Acad Sci USA **93**: 14618–14622

**Roger AJ, Svärd SG, Tovar J, Clark CG, Smith MW, Gillin FD, Sogin ML** (1998) A mitochondrial-like chaperonin 60 gene in *Giardia lamblia*: evidence that diplomonads once harbored an endosymbiont related to the progenitor of mitochondria. Proc Natl Acad Sci USA **95**: 229–234

**Sogin ML** (1997) History assignment: when was the mitochondrion founded? Curr Opin Genet Dev **6**: 792–799

**Sogin ML, Silberman JD** (1998) Evolution of the protists and protistan parasites from the perspective of molecular systematics. Int J Parasitol **28**: 11–20

**Soltys BJ, Falah M, Gupta RS** (1996) Identification of endoplasmic reticulum in the primitive eukaryote *Giardia lamblia* using cryoelectron microscopy and antibody to Bip. J Cell Sci **109**: 1909–1917

**Takizawa PA, Yucel JK, Veit B, Faulkner DJ, Deerinck T, Soto G, Ellisman M, Malhotra V** (1993) Complete vesiculation of Golgi membranes and inhibition of protein transport by a novel sea sponge metabolite, ilimaquinone. Cell **73**: 1079–1090